Automatic quality control of telemetric rain gauge data providing quantitative quality information (RainGaugeQC)

Katarzyna Ośródka[1], Irena Otop[2], Jan Szturc[1]

[1]Centre of Meteorological Modelling, Institute of Meteorology and Water Management – National Research Institute, PL 01-673 Warszawa, Podleśna 61, Poland
[2]Research and Development Centre, Institute of Meteorology and Water Management – National Research Institute, PL 01-673 Warszawa, Podleśna 61, Poland

Correspondence to: Jan Szturc (jan.szturc@imgw.pl)

Abstract. The RainGaugeQC scheme described in this paper is intended for real-time quality control of telemetric rain gauge data. It consists of several checks: detection of exceedance of the natural limit and climate-based threshold, and checking of the conformity of rain gauge and radar observations, the consistency of time series from heated and unheated sensors, and the spatial consistency of adjacent gauges. The proposed approach is focused on assessing the reliability of individual rain gauge observations. A quantitative indicator of reliability, called the quality index (*QI*), describes the quality of each measurement as a number in the range from 0.0 (completely unreliable measurement) to 1.0 (perfect measurement). The *QI* of a measurement which fails any check is lowered, and only a measurement very likely to be erroneous is replaced with a "no data" value. The performance of this scheme has been evaluated by analysing the spatial distribution of the precipitation field and comparing it with precipitation observations and estimates provided by other techniques. The effectiveness of the RainGaugeQC scheme was also analysed in terms of the statistics of *QI* reduction. The quality information provided is very useful in further applications of rain gauge data. The scheme is used operationally by the Polish national meteorological and hydrological service (Institute of Meteorology and Water Management – National Research Institute).

1 Introduction

The accuracy of telemetric rain gauge data is vital both for scientific research and for real-time modelling. Reliable precipitation measurements with high temporal and spatial resolution are essential input data for numerous operational applications in meteorology and hydrology, such as quantitative precipitation estimation (QPE), nowcasting, real-time initial conditions for numerical weather prediction, hydrological modelling, etc. Incorrect values may affect the results of these applications; this applies especially to unreasonably high or false zero precipitation values.

In recent decades, the number of automated weather station networks providing measurements with high temporal resolutions (e.g. 1-, 5-, or 10-minute) has rapidly increased. Consequently, procedures for data quality control (QC) have developed from manual or semiautomatic to fully automatic checks that provide relevant quality information, such as quality flags or quality indices (Lewis et al., 2021). However, in the case of precipitation, the effectiveness of automatic quality control methods has been proven to be much lower than in the case of other meteorological parameters (You et al., 2007). The key issue is the spatiotemporal variability of the precipitation field, which can be very intermittent and small-scale, depends strongly on the type of precipitation (e.g. convective or frontal), and also depends on topographic variables in mountainous areas with complex terrain (Scherrer et al., 2011).

This paper presents the RainGaugeQC software, which is a package of automatic QC procedures, developed at the Institute of Meteorology and Water Management – National Research Institute (IMGW), which operates the Polish national meteorological and hydrological service. The scheme focuses on telemetric rain gauge measurements, and is designed to identify erroneous or suspicious data and to assign a quality index (*QI*) to the individual measurements. The RainGaugeQC

was designed specifically for quality control of sub-hourly rain gauge data. This is a particularly challenging task because of the higher spatial variability and lower spatial consistency of such data (Villalobos Herrera et al., 2022).

1.1 Sources of errors in rain gauge data

Ground rain gauge measurements, like other observations, are affected by different types of errors, usually classified as random, systematic and gross errors. Random errors vary in an unpredictable manner, while systematic errors remain constant or vary in a predictable way, and can often be reduced. Gross errors are characterised by rare occurrence and large magnitude (WMO-No. 488, 2017).

Problems relating to the accuracy of precipitation measurement have been well documented (e.g. Sevruk, 1996; Habib et al., 2001; Golz et. al., 2005; Sieck et al., 2007; Sevruk et al., 2009). The magnitude of measurement errors depends on many factors, including weather conditions at the collector, the location of the rain gauge, and the gauge type. The most significant measurement errors are related to wind (Sevruk et al., 2009; Rasmussen et al., 2012; Martinaitis et al., 2015). Wind-induced losses mainly depend on wind speed and turbulence, as well as the type of precipitation (e.g. rain, mixed snow and rain, or snow). The measurement error is usually greater for solid than for liquid precipitation (WMO-No. 8, 2018). Because of slow falling, snow hydrometers are more susceptible to deflection by wind-induced turbulence around the gauge, making snowfall measurements prone to large systematic errors (Rasmussen et al., 2012). In windy conditions, the underestimation of snowfall accumulation frequently ranges from 20% to 50% or even higher, and additionally depends on other variables, such as exposure and the type of rain gauge (Rasmussen et al., 2012; Buisán et al., 2017; Grossi et al., 2017). Other systematic error sources are related to physical processes, such as evaporation from a bucket, wetting, and splashing. All such errors are typically referred to as catching losses.

Additional difficulties occur in winter precipitation measurements as a result of snow collecting on the gauge or snow accumulating within wind shields, either of which can completely or partially block the gauge orifice (Goodison et al., 1998; Rasmussen et al., 2012; Martinaitis et al., 2015; Kochendorfer et al., 2020). In consequence, Martinaitis et al. (2015) identified a secondary but important impact from gauges that had become partially or completely stuck during winter precipitation events. Thawing due to increased surface ambient temperatures resulted in gauges reporting false non-zero precipitation after having collected solid precipitation. These impacts became increasingly complex when rainfall occurred simultaneously with the thawing of accumulated solid precipitation.

Moreover, the accuracy of precipitation measurements may be affected by improper exposure of the gauge, site altitude, shielding or obstacles (e.g. trees, buildings) near the rain gauge, the impact of topographic variables in complex areas, and the seeder–feeder effect (when precipitation from an upper-level cloud falls through a lower-level orographic stratus cloud capping a small mountain) (Førland et al., 1996; Sevruk and Nevenic, 1998).

Additionally, mechanical problems specific to each type of rain gauge influence the accuracy of precipitation measurements. Tipping bucket rain gauges are subject to random errors related to partial or total blockages of the mechanism due to accumulated mineral or biological particulates: dust, insects, blown grass, etc. (Sevruk, 1996; Upton and Rahimi, 2003). In consequence, even partial clogging of the gauge can result in erroneous estimates of the intensity and duration of rainfall. Another specific problem with tipping bucket rain gauges relates to high-frequency bucket tips (double tips), which lead to the recording of spurious high rainfall intensities, while on the other hand very slow tips (i.e. a limited tipping rate) may result in misleading underestimates of rain rates (Upton and Rahimi, 2003; Shedekar et al., 2016).

In the case of weighing gauges, the most relevant sampling errors are related to the response time of the measurement system and the consequent systematic delay in assessing the exact weight of the accumulated precipitation in the container, especially in the case of high resolution (e.g. a 1-minute time resolution). Sampling errors may also affect the measurement of low-intensity rain (Colli et al., 2013).

80 Electronic weighing precipitation gauges are less susceptible to evaporation losses than tipping bucket gauges and have
81 better accuracy in assessing the beginning of snowfall events. A heated tipping bucket gauge starts recording with a delay due
82 to the time needed to melt the snow and fill the first tip, and measures less precipitation due to heating-related losses (Savina
83 et al., 2012).

84 Furthermore, precipitation measurements may be affected by gross errors, mainly caused by the malfunctioning of
85 measurement devices, or occurring during data transmission.

1.2 Approaches to quality control of rain gauge data

87 Quality control is a vital part of data processing in order to achieve a certain standard for international data exchange. The
88 World Meteorological Organisation (WMO) recommends initially to perform real-time basic QC of raw data at sensor level,
89 then near-real-time QC, and finally non-real-time extended QC (semi-automatic) at the headquarters (WMO-No. 488, 2017).
90 Performing QC at various stages of data processing makes it possible to identify the majority of errors in the dataset.

91 Generally speaking, some precipitation data QC checks consider each single observation separately (Upton and Rahimi,
92 2003; Taylor and Loescher, 2013; Blenkinsop et al., 2017), whereas more complex ones also take into account data from
93 neighbouring stations (Steinacker et al., 2011; Scherrer et al., 2011) or multi-source data, such as weather radar data (Yeung
94 al., 2014; Baserud et al., 2020) and output from a numerical weather prediction model (Qi et al., 2016). Recently, due to the
95 increased utilisation of crowdsourced observations, specific QC methods applicable for this type of precipitation data have
96 been developed (de Vos et al., 2019; Bárdossy et al., 2021; Niu et al., 2021).

97 For assessing the reliability of observations, several approaches are adopted. In practice, various measures of the quality
98 of precipitation data are used. They indicate the reliability of individual sensors resulting from measurement precision, which
99 is strongly conditioned by construction and technology (Førland et al., 1996), location, current meteorological conditions
100 (wind, temperature), etc. Often, flags describing the quality of the data are used qualitatively; for example, the WMO
101 recommends a scheme of five quality flags, defined as good, inconsistent, doubtful, erroneous, and missing (WMO-No. 488,
102 2017, p. 201).

103 In the simple approach to QC outputs, the only possible result is the acceptance or rejection of particular observations.
104 An observation that passes all of the checks is flagged as correct. If an observation fails a check, it is flagged as incorrect and
105 does not undergo the remaining checks (Baserud et al., 2020); however, it is possible to retrieve information on which test was
106 failed for each observation. Some QC schemes integrate the results of individual QC checks to generate a final flag for each
107 observation. In this case an adjustment test or specially designed rule base is applied to minimise the number of correct
108 observations that are flagged as "erroneous". For example, if an observation failed a climate-based range test but passed the
109 spatial check, then an adjustment test may reduce the severity of the flag obtained from the climate-based range check (Fiebrich
110 et al., 2010; Lewis et al., 2018; 2021).

111 In another approach, after failing specific checks the measured values are not removed, but corrected. Such a method
112 may be used to replace suspicious data with values obtained from interpolation data from neighbouring stations (Michelson,
113 2004), but it does not provide any additional information. Also, the use of data from other measurement systems is not a
114 satisfactory solution, as these data are generally inconsistent with each other due to their different spatial distributions.
115 Generally, the correction of measured values can give unreliable results due to the high level of arbitrariness.

116 Recently, machine learning using artificial neural networks has been employed as a tool for automated quality control
117 as well as for the correction of errors and reconstruction of missing values in precipitation data (Moslemi and Joksimovic,
118 2018).

119 Quantitative indicators based on various forms of quality indicator can also be used, describing the quality of the
120 observations expressed in numbers, most often in the range from 0.0 (completely unreliable measurement) to 1.0 (perfect
121 measurement) (Einfalt et al., 2010; Szturc et al., 2022). This approach is adopted in the QC scheme described in this paper. In

the developed RainGaugeQC scheme, the quality of uncertain measurements is lowered and only measurements very likely to be erroneous are removed – they are replaced with "no data" values. The advantage of this approach is that the quality information can be very useful in further applications. For example, it is employed in quality-based spatial interpolation of rain gauge data and in merging observations from different measurement techniques (e.g. Jurczyk et al., 2020). It seems optimal to take into account quantitative information about the quality of individual measurements in such a way that the more uncertain data are assigned a lower weight than more reliable data.

1.3 Structure of the paper

The paper is structured as follows. After section 1, section 2 briefly describes the rain gauge data on which the RainGaugeQC scheme proposed in the paper was developed and calibrated, as well as the radar data used as auxiliary data in this scheme. In section 3, the checks that constitute the RainGaugeQC system are presented (their detailed descriptions are included in the appendices). Section 4 presents and discusses specific examples of the scheme's performance and a general analysis of its operation. The article ends with a list of conclusions resulting from the operational use of the RainGaugeQC scheme at IMGW (section 5).

2 Data sources

2.1 Rain station network in Poland

The Polish national meteorological and hydrological service, provided by IMGW, operates a nationwide meteorological telemetric network which consists of 503 rain stations equipped mainly with tipping bucket sensors (Fig. 1). At the synoptic stations, SEBA Hydrometrie (https://www.seba-hydrometrie.com/) RG-50 devices are installed, whereas precipitation stations use mainly the Met One Instruments (https://metone.com/) 60030 and 60030H devices (unheated and heated, respectively). Telemetric precipitation measurements are available with a 10-minute time resolution: all year round for heated sensors, and in the warm part of the year – from April to October – for unheated ones.
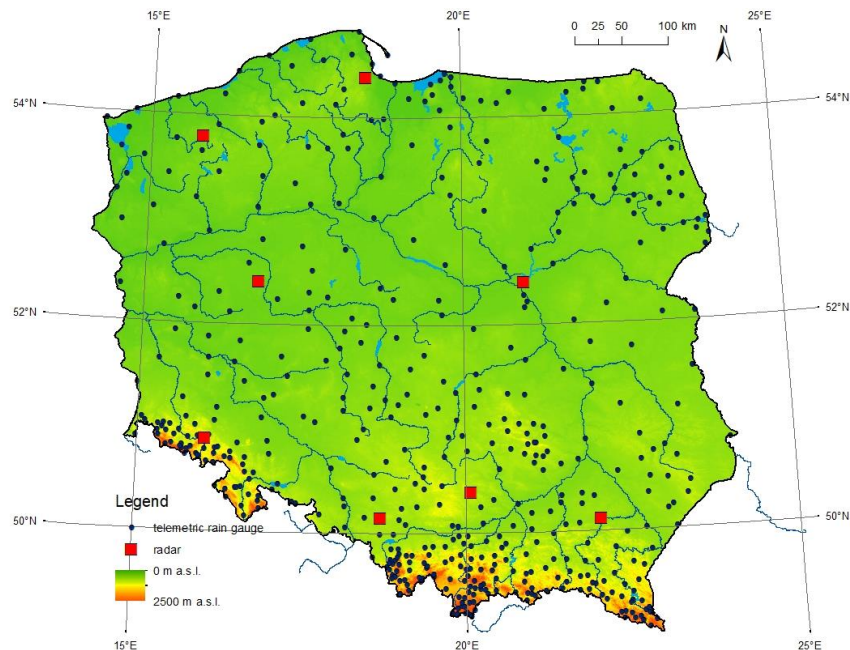

Figure 1: Networks of telemetric rain stations and weather radars in Poland.

148   The reliability of individual rain gauge depends on the type of the gauge and its location, and changes with time. The
149   network's tipping bucket devices often malfunction, and moreover these sensors lower the precipitation values by an average
150   of about 8–20% (Urban and Strug, 2021).

151   Fig. 2 shows the relationships between measurements of 10-minute precipitation accumulations from unheated and
152   heated sensors on two sample rain stations: in Dzierżoniów, located in the foothills area, during July 2021 (left), and in Nowa
153   Wieś Podgórna, located in the lowland Wielkopolska (Greater Poland) region in central Poland, during June 2021 (right). Both
154   stations are equipped with two tipping bucket sensors. The correlation coefficient calculated for pairs of values in which at
155   least one is different from zero is extremely high for Dzierżoniów, being equal to 0.997 (Fig. 2a), while for Nowa Wieś
156   Podgórna it is only 0.694 (Fig. 2b), a fairly low result caused by very large differences between the values measured
157   simultaneously by the two sensors at the same location. The reason for such low correlation may be that tipping bucket gauges
158   are susceptible to frequent sensor failures.

159   Generally, the left graph of Fig. 2 corresponds to a well-functioning rain station, and the right graph corresponds to a
160   rain station with one or both sensors not functioning correctly, therefore they require effective quality control. It is shown in
161   section 4.3, concerning an example case study, how the quality control scheme presented in this paper worked on these
162   obviously incorrect measurements.

163
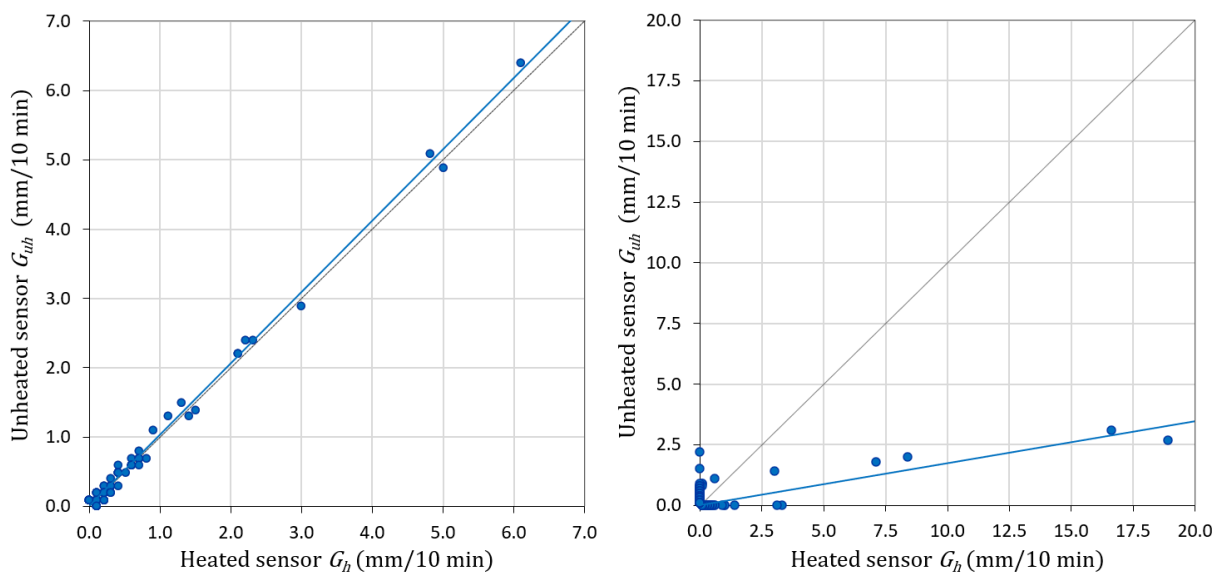
164

165
166
167   **Figure 2: Relationships between observations of 10-minute precipitation accumulations measured with tipping bucket rain stations**
168   **equipped with two sensors – unheated and heated – in Dzierżoniów during July 2021 (left) and in Nowa Wieś Podgórna during June**
169   **2021 (right). The blue lines mark the trends of these relationships. The data from 3 rain stations showed at the bottom map are**
170   **discussed in the examples.**

171   **2.2 Weather radar data**

172   Weather radar data are employed in the RainGaugeQC scheme as auxiliary data to verify rain gauge observations. They are
173   generated by the Polish radar network POLRAD, which consists of eight C-band Doppler radars from Leonardo Germany
174   GmbH (formerly Gematronik and Selex) (Szturc et al., 2018). Three of them are dual-polarisation radars, and work is currently
175   underway on upgrading all the radars, including dual polarization functionality. Three- and two-dimensional radar products

5

are generated by Rainbow 5 software every 10 min, with a 1 km spatial resolution within a 215 km range. The Marshall–Palmer formula is used to transform the reflectivity values measured by radar into the precipitation rate, this being the most common form of such a relationship (Neuper and Ehret, 2019). The data are quality controlled by the dedicated RADVOL-QC system developed at IMGW (Ośródka et al., 2014; Ośródka and Szturc, 2022). The system also generates quality fields, $QI(R)$, based on analyses of particular errors disturbing radar data.

2.3. Other data

In addition, the fields of the following precipitation estimates were used for the case studies:

- satellite precipitation fields determined from various NWC-SAF (Satellite Application Facilities on Support to Nowcasting and Very Short Range Forecasting) products based on Meteosat data (Jurczyk et al., 2020),
- QPE fields produced by the RainGRS system, which operationally combines precipitation data from rain gauges, weather radar and meteorological satellites, based on conditional merging and additionally taking quality information into account (Jurczyk et al., 2020).

3 General description of the developed quality control scheme

3.1 Set of RainGaugeQC algorithms

A shortened version of the description of the algorithms used in the scheme was presented in works by Otop et al. (2018) and Jurczyk et al. (2020). This section and the related appendices provide a full description of the developed algorithms. All parameters defined here were optimised for 10-minute precipitation accumulations (mm/10 min).

Table 1. List of sequential checks for precipitation QC.

ID	Abbreviation	Name	Main approach	Result of the check
1	GEC	Gross Error Check	Detection of exceedance of the natural limit	Removal of incorrect values
2	RC	Range Check	Detection of exceedance of climate-based threshold at an individual gauge	QI reduction for suspiciously high precipitation value
3	RCC	Radar Conformity Check	Checking of the conformity of rain gauge and radar observations	Removal of false "no precipitation" data. For false precipitation reports, QI reduction depending on $SF(G_h, G_{uh})$ and location
4	TCC	Temporal Consistency Check	Checking of the consistency of time series from heated and unheated sensors	QI reduction for inconsistent sensors
5	SCC	Spatial Consistency Check	Checking of the spatial consistency of adjacent gauges	QI reduction for outliers depending on the inconsistency level

The rain gauge quality control procedure developed at IMGW consists of several checks (Table 1). Firstly, simple plausibility tests – the gross error check and range check – are performed on a single measurement. Then more complex checks are performed, using data from both measurement sensors at the site and data from weather radars.

Before the checks, each sensor is assigned the perfect QI value (1.0). In case of failure of a particular check, the QI value is decreased by a specified value. If the final QI value (after all of the checks) is very weak (≤ 0.0), the sensor is considered useless and the measurement value is replaced with "no data".

The sensor which obtained a higher final quality index is used for further applications, but if both sensors are of the same quality, then the heated sensor is taken.

3.2 Similarity function (SF)

It is useful to introduce a tool to check the similarity of two sums of precipitation. For this purpose a similarity function (SF) has been proposed and is used in some of the checks. The function $SF(G_h, G_{uh})$, comparing precipitation data from two sensors

207 G_h and G_{uh} (heated and unheated) installed at the same rain station G in order to check whether the measured values are
208 consistent, is defined as follows:

209 If ($G_h < 1.0$ mm or $G_{uh} < 1.0$ mm), then

210   if ($|G_h - G_{uh}| < 1.0$ mm), then $SF(G_h, G_{uh}) =$ "true"   (1)

211   else $SF(G_h, G_{uh}) =$ "false"

212 whereas:

213 If ($G_h \geq 1.0$ mm and $G_{uh} \geq 1.0$ mm), then

214   if $\left(0.5 < \frac{G_h}{G_{uh}} < 2.0 \text{ or } |G_h - G_{uh}| < 1.0 \text{ mm}\right)$, then $SF(G_h, G_{uh}) =$ "true"   (2)

215   else $SF(G_h, G_{uh}) =$ "false"

216   In the above formulae, precipitation units are given in "mm", but they may refer to different accumulation periods, for
217 example, mm per 10 minutes (mm/10 min) or 1 hour.
218   The result of the use of *SF* to assess the similarity of measurements between two sensors (heated and unheated) in rain
219 stations is presented in Fig 3. The graph shows example data for one day, 22 May 2019, obtained from all measuring stations.
220 It is indicated which measurements from the two sensors are shown by the *SF* function to be similar (marked blue) and which
221 are not similar (marked brown). The two blue dashed lines delimit the area in which the values measured by the unheated and
222 heated sensors are similar according to the *SF* function.

223
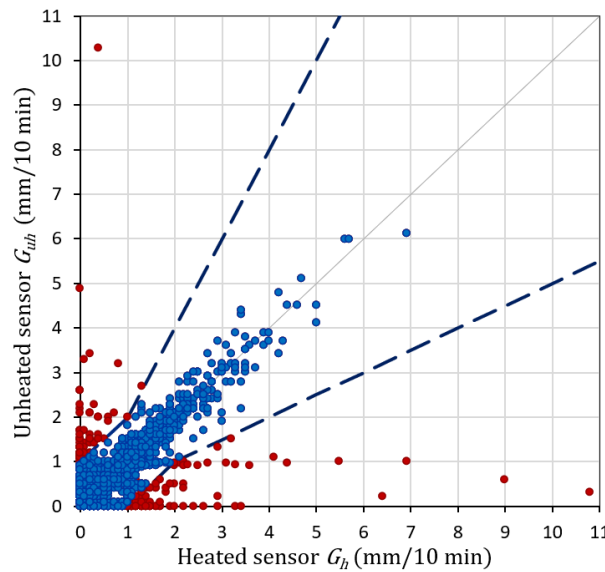
224
225
226 **Figure 3: Precipitation data from G_{uh} and G_h sensors that are similar (blue) and not similar (brown). The similarity of the**
227 **measurements from all rain stations on 22 May 2019 was determined using the similarity function SF. The two dashed lines delimit**
228 **the area in which the measurements are considered similar.**

229 **3.3 Gross Error Check (GEC)**

230 GEC is a preliminary check to identify gross errors which have a strong effect on the further analyses. These errors are mainly
231 caused by the malfunctioning of measurement devices or by mistakes occurring during data transmission or processing
232 (Steinacker et al., 2011). GEC examines whether the rain gauge measurement is within the physically acceptable range limits:
233 not less than 0 mm and not above 56 mm/10 min (i.e. 51 dBZ). The upper limit was determined on the basis of a formula

7

234 developed to estimate the maximum reliable precipitation for various durations in Poland (Burszta-Adamiak et al., 2019). A

235 measurement that fails the check is rejected from further processing.

3.4 Range Check (RC)

237 RC verifies a single measurement against a threshold value, which is based on local climatological data with respect to seasonal

238 variation of observations in the specific location of the rain station. This test identifies data as implausible when they exceed

239 the expected maximum value, that is, the threshold empirically estimated from long-term climatological data. It is essential to

240 ensure reliable values of the threshold, because, for example, too low a threshold may cause extreme values of precipitation to

241 fail the test (Taylor and Loescher, 2013). Therefore, Fiebrich et al. (2010) recommend developing regionally specific

242 thresholds for the test. In the proposed QC procedure, the thresholds were defined as 10-minute precipitation values with a 1%

243 probability of being exceeded, determined separately for warm and cold seasons. These values were calculated for each

244 telemetric station, based on the statistical distribution of 10-minute accumulations in a 30-year time series (1986-2015). In the

245 case that the examined measurement exceeds the relevant threshold value, it is treated as suspicious and its *QI* is reduced by

246 0.25.

3.5 Radar Conformity Check (RCC)

248 RCC is performed to identify false precipitation – false zero and false gauge-reported precipitation measurements – on the

249 basis of radar data, which quite reliably indicate the spatial distribution of precipitation. RCC compares each gauge observation

250 lower than 0.2 mm/10 min with radar observations at the gauge location and its surrounding of 3 pixels x 3 pixels (the pixel

251 size is 1 km x 1 km). If the radar data for the vicinity of the station are above a predefined threshold, then a "no precipitation"

252 result measured by the sensor is assumed to be false and the *QI* is reduced to 0.0.

253 On the other hand, the RCC compares every sensor observation $G > 0$ mm/10 min with radar observations at the gauge

254 location and its neighbouring of 3 pixels x 3 pixels. If the radar data is of a quality $QI(R)$ above a predefined threshold and

255 indicates "no precipitation" (0 mm), then the precipitation measured by the sensor is assumed to be false and the *QI* of that

256 observation is reduced. The reduction depends on whether data are available from one or two sensors, on their similarity, and

257 on the gauge location. The following regions based on altitude are distinguished: lowlands (areas below 300 m a.s.l.). foothills

258 (between 300 and 600 m a.s.l.), and mountainous (areas above 600 m a.s.l.).

259 For a detailed description of the RCC algorithm and the criteria for determining the reduction of *QI*, see Appendix 1.

3.6 Temporal Consistency Check (TCC)

261 This check, in the form described below, is possible only when two sensors are installed at each measuring station, most often

262 heated and unheated, as is currently the case in the IMGW network. If this is not the case, then a method commonly used in

263 quality control of various meteorological quantities is to check the time continuity of the measured values. For some types of

264 meteorological data the time consistency checks are efficient; however, in the case of precipitation data, this check would

265 eliminate not only all questionable data but also a large amount of true data, in particular extreme values, because of the high

266 variability of precipitation (WMO-No. 305, 1993, p. VI.21, VI.23).

267 The first step of this check is performed to detect a clogged sensor, which occurs if the same value is repeated over a

268 certain period of time. In this case, the sensor's quality is reduced to 0.0.

269 In the next step, pairs of rain gauge sensors (G_h, G_{uh}) are tested for the existence of large differences between them.

270 This check requires measurements from both rain gauge sensors at the same location, and can thus be conducted only in the

271 warm half of the year, because only then two time series from the same station are available. In this procedure, if the number

272 of measurement pairs is sufficient, they are accumulated and their similarity is checked using the SF function (see section 3.2).

273 If the sums differ, the data from both sensors have failed the TCC check and their quality is reduced.

274   For a detailed description of the TCC algorithm see Appendix 2.

275 **3.7 Spatial Consistency Check (SCC)**

276 SCC is applied to identify outliers based on a comparison with neighbouring stations. Additionally, radar data are introduced

277 to assess the level of *QI* reduction for outliers.

278   There are several steps in the operational procedure for SCC. Firstly, the domain area is divided into basic subdomains

279 with a spatial resolution of 100 km x 100 km. For each subdomain, a set of percentiles of rain gauge data and the median

280 absolute deviation (*MAD*) are calculated.

281   The criterion for the spatial consistency of an individual sensor is implemented based on the index *D*, calculated using

282 the formula of Kondragunta and Shrestha (2006). This index is compared with the threshold values defined by set of percentiles

283 of the index *D*, making it possible to determine the different classes of outliers. The check is repeated for subdomains obtained

284 by making shifts of 25 km in all four directions. If the sensor value is identified as an outlier in the basic subdomain and in the

285 shifted subdomains, the sensor is detected as an outlier and a further procedure is applied to assess the relevant quality

286 reduction.

287   For each detected outlier, two criteria are checked: (i) if data from both sensors are available for a given rain gauge and

288 they are similar, i.e. *SF* (G_h, G_{uh}) = "true", and (ii) if the data passed the TCC test. If both criteria are met, then the *QI* for the

289 sensor is not reduced. Otherwise, for additional verification, radar data in a grid of 5 pixels x 5 pixels around the gauge location

290 are considered if they are of good quality. In this case the reduction of the *QI* value depends on the class of the outlier (weak,

291 medium, or strong) and the magnitude of the disparity with the radar data (the limitation imposed on the magnitude of this

292 disparity has been determined empirically).

293   A detailed description of the SCC algorithm and the criteria for reduction of the *QI* value are given in Appendix 3.

294   The check may optionally analyse data from both sensors together or separately, and may include or not data from the

295 previous time step. It was investigated how these two settings influence the performance of the check.

296   Fig. 4 presents graphs showing the percentage of data with reduced *QI* values, as a result of analysing the spatial

297 conformity of data from two types of sensors (unheated and heated) separately or together. The obtained sample results

298 generally showed large variation; however, the numbers of strong outliers increased significantly (about 2.35% versus 0.6%)

299 when the two types of sensors were analysed separately – in that case the algorithm appears much less tolerant.

300
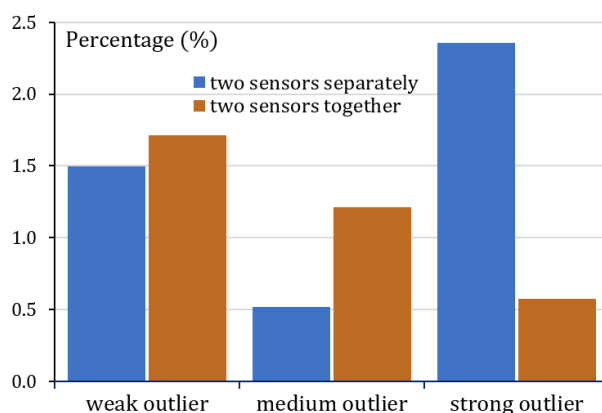
301
302
303 **Figure 4: Percentage of classes of outliers (weak, medium, and strong) when analysing the data from two types of sensors (unheated**
304 **and heated) separately (blue) or together (brown). Data from 22 May 2019.**

If the algorithm takes into account data not only from the current time step, but also from 10 minutes ago (both sensors analysed together), then these numbers are slightly higher for weak and medium outliers and slightly lower for strong ones. The latter indicates that the inclusion of data from the previous time step makes the algorithm more tolerant.. The percentage of the data belonging to all classes of outliers together was slightly over 3% (Fig. 5), and for particular classes varies from about 1.5–1.7% for the weak to about 0.6–0.9% for the strong outliers.
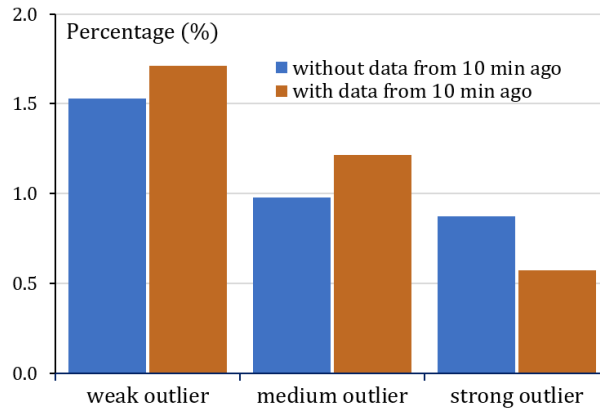
Figure 5: Percentage of classes of outliers (weak, medium, and strong) when analysing measurements from the given time only (blue) and also from the previous time step (brown). Data from two days: 20–21 June 2020.

In the RainGaugeQC scheme currently used by IMGW in real time, in the SCC check both types of sensors are analysed together, also taking account of the data from the previous time step.

3.8 Quality index of spatially distributed rain gauge data

In most applications of rain gauge data, spatial interpolation of the point data is required and this procedure can be carried out by any of a number of commonly known methods. However, it is not enough to spatially interpolate the *QI* values assigned to individual rain gauges. It is also necessary to take into account the fact that the uncertainty of the estimated field increases very quickly with increasing distance from the nearest rain gauge. Therefore, the quality field for the spatially distributed precipitation data depends on two factors: the *QI* point values for individual rain gauges (denoted by the *QI* with the index "*p*") and a factor that depends linearly on the distance from the nearest rain gauge (with the index "*d*").

The precipitation and *QI* point values from rain stations are spatially interpolated simultaneously by the same method using the same parameters, so in both cases there are the same contributions from the individual rain gauges. Hence the obtained quality field $QI(G_{\text{int}}(x,y))_p$ is completely consistent with precipitation field $(G_{\text{int}}(x,y))$. In the case of the operational scheme used by IMGW, ordinary kriging is applied, where the domain of 900 km x 800 km is divided into 16 subdomains of 225 km x 200 km and interpolation is performed separately in each of them.

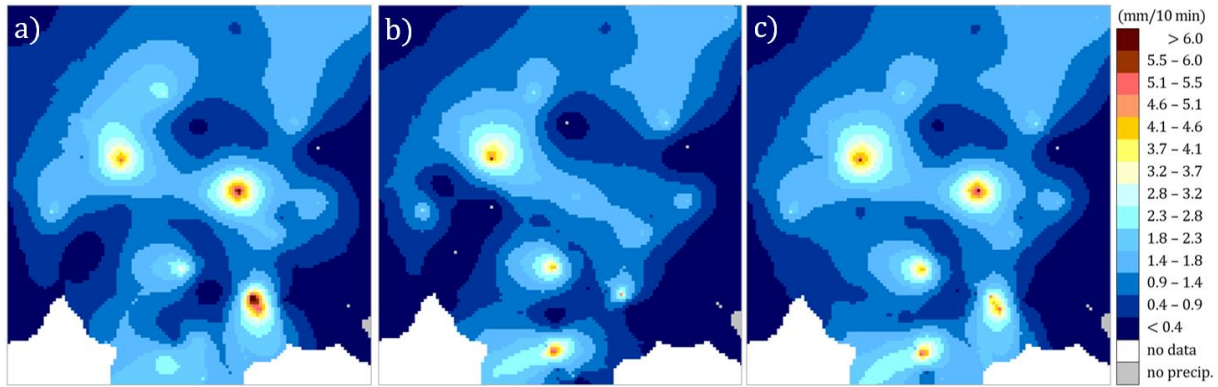The factor related to the distance from the rain gauges $QI(G_{\text{int}}(x,y))_d$ takes into account the decrease in the quality of the rainfall field depending on the distance $d(x,y)$ to the nearest rain gauge. The distance factor for each pixel is calculated from the linear formula:

$$QI(G_{int}(x,y))_d = \frac{d_{max} - d(x,y)}{d_{max}} \tag{3}$$

where $d_{\max}$ is the limit value of the distance to the nearest rain gauge, above which the quality at that pixel is assigned a value of zero (the adopted limit is 100 km).

The field of the final quality index for the rain gauge-based precipitation field is calculated from the product of the two above factors:

$$QI(G_{\text{int}}(x,y)) = QI(G_{\text{int}}(x,y))_p \cdot QI(G_{\text{int}}(x,y))_d \tag{4}$$

338 **4 Examples of QC scheme operation**

339 **4.1 Influence of differences in values from two sensors on precipitation field estimation**


340
341
342 **Figure 6: Spatially interpolated rain station data obtained from: (a) unheated and (b) heated sensors, and (c) after quality control**
343 **(considered optimal). Data from 5 August 2021, 17:40 UTC, fragment from the Polish domain (240 km x 250 km).**

344 In the example presented in Fig. 6, it can be seen that the data from the two sensors can sometimes be significantly different.

345 In simpler solutions the final rainfall field can be generated by taking the mean or the higher values of the two sensors at the

346 same location, and both of these approaches can be justified depending on the final application of the data. The approach used

347 in the RainGaugeQC scheme makes it possible to choose the better value according to defined checks. Moreover, it enables to

348 apply that precipitation value along with the relevant *QI* value in quality-based interpolation algorithms which generate the

349 optimal rain gauge field.

350 **4.2 Result of the performance of the QC scheme after the introduction of erroneous values**

351 Fig. 7 illustrates the performance of the proposed QC scheme. If the rain gauge data are not subjected to QC algorithms, then

352 two alternative data sets can be considered: from unheated (Fig. 7a) and heated (Fig. 7b) sensors. The third diagram shows an

353 example of data disturbed with an artificial value of 10 mm/10 min at the heated sensor of the Siercza rain station (Fig. 7c),

354 which is marked with a red circle in all diagrams. Location of the Siercza rain station is shown in Fig. 2 (bottom).

355
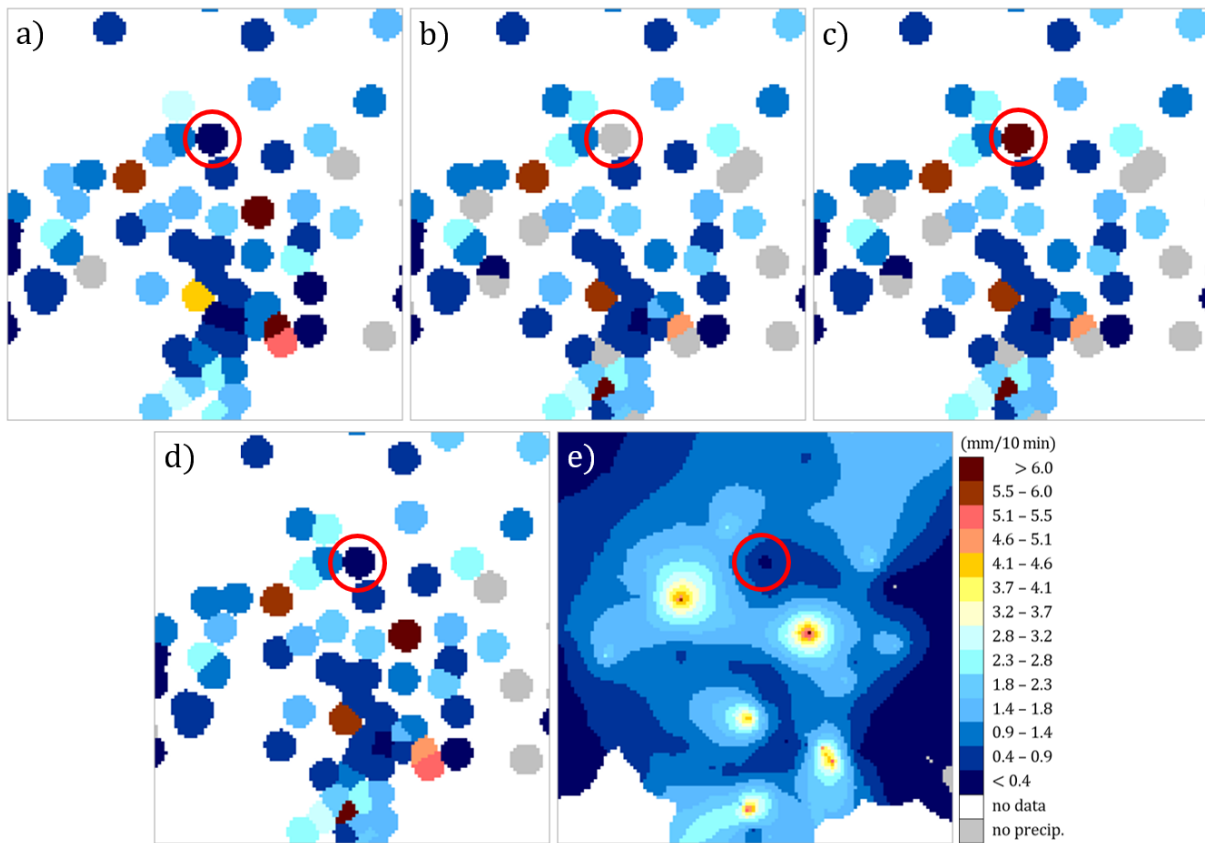
Fig. 7. Example of the RainGaugeQC performance after the introduction of erroneous precipitation value: (a) original rain gauge data from unheated sensors (G_{uh}) (in all fields the Siercza rain station is marked with a red circle), (b) original data from heated sensors (G_h), (c) data from heated sensors disturbed with an artificial value at Siercza (10 mm/10 min), (d) rain gauge data after quality control, and (e) after spatial interpolation. Data from 5 August, 2021, 17:40 UTC, fragment from the Polish domain (240 km x 250 km).

Fig. 7d shows the values from individual rain stations after quality control, and Fig. 7e shows the precipitation field after spatial interpolation using the ordinary kriging technique (this field is identical to the one shown in Fig. 6c).. As these images show, the precipitation values obtained after data quality control are some mixture of those data from both sensors that passed the QC with higher QI (see section 3.1). The Siercza rain station, marked with a red circle, serves here as an example of a station with incorrect measurement (the original values were 0.2 and 0.0 mm/10 min for unheated and heated sensors, respectively). The erroneous value of 10 mm/10 min was eliminated as a result of the QC algorithms, so the rainfall value for this rain station after QC is 0.2 mm/10 min measured by the unheated sensor.

4.3 Example for Nowa Wieś Podgórna rain station from 22 June 2021, 13:30 UTC

An example of a rain station with low-quality measurements, taken from the Nowa Wieś Podgórna rain station during June 2021, is shown in Fig. 2b (section 2.1). The low quality is evidenced by large differences between the values measured with heated and unheated sensors: the heated sensor recorded much higher 10-minute precipitation accumulations than the unheated one. The data from 22 June 2021, 13:30 UTC are analysed in detail below. The heated sensor of the Nowa Wieś Podgórna rain station reported a very high rainfall of 18.9 mm/10 min, whereas the unheated one reported only 2.7 mm/10 min (Table 2). If QC is not performed, then the heated sensor is generally considered the primary sensor as it operates all year round. The precipitation field resulting from the interpolation of rain gauge data without QC obtained by the ordinary kriging method is shown in Fig. 8a.

12
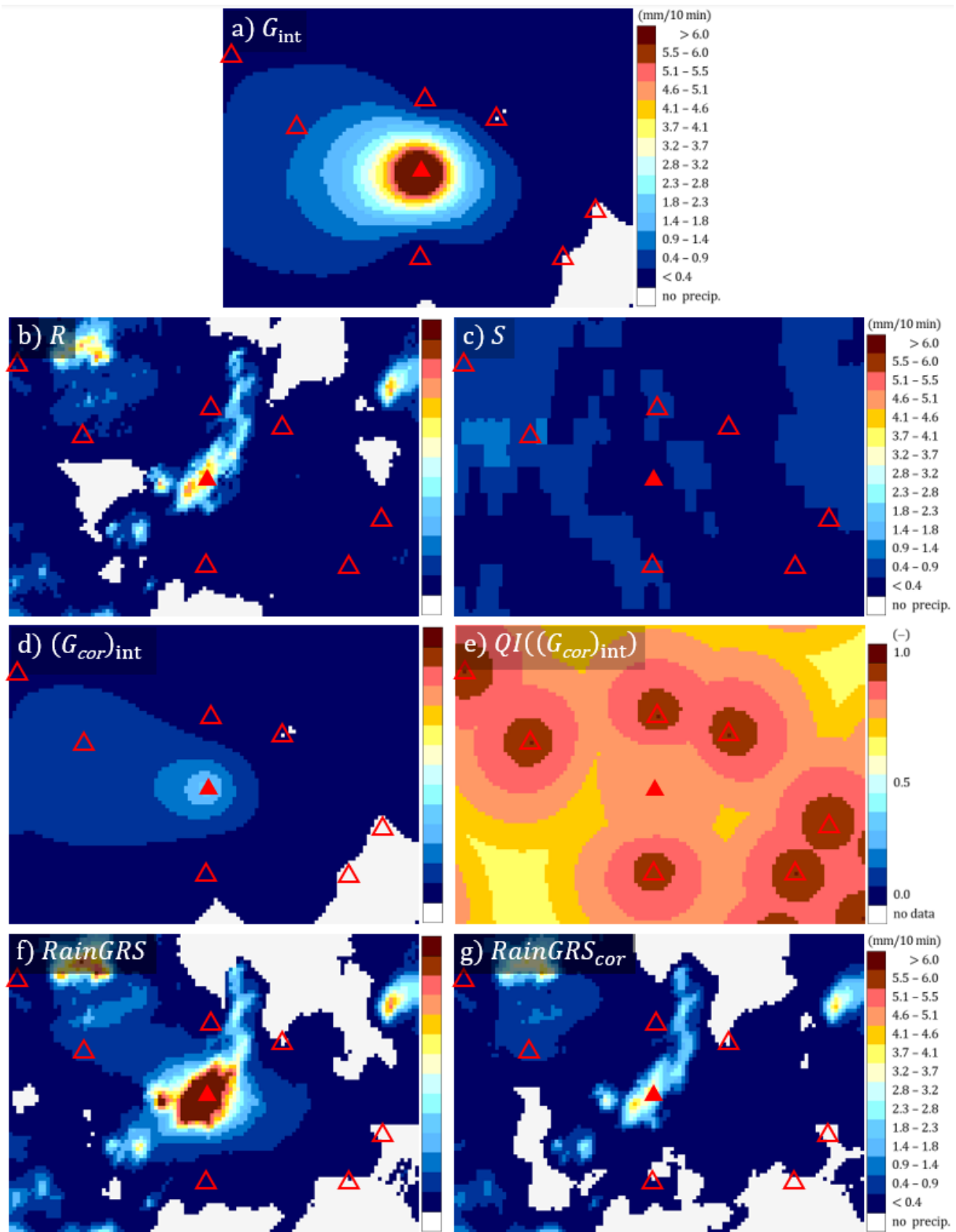
Figure 8: Various fields of 10-minute precipitation accumulation (in mm/10 min) in the vicinity of the Nowa Wieś Podgórna rain station (marked with a red triangle; the locations of other rain stations are marked with empty triangles): a) spatially interpolated field from rain gauge data without QC (G_{int}), b) radar-based precipitation field (R), c) satellite-based precipitation field (S), d) spatially interpolated field from rain gauge data after QC ((G_{cor})$_{int}$), e) QI field for the precipitation field from rain gauge data after QC ($QI(($G_{cor}$)_{int})$), f) multi-source precipitation field ($RainGRS$) obtained from raw rain gauge data, g) multi-source precipitation field ($RainGRS_{cor}$) obtained from rain gauge data after QC. Data from 22 June 2021, 13:30 UTC, fragment from the Polish domain (110 km x 80 km).

In order to diagnose the large difference between the two sensors, a detailed investigation of the situation was performed based on precipitation data from other sources. The radar composite map from the SRI (surface rainfall intensity) product showed 3.95 mm/10 min at this location (Fig. 8b), which is much closer to the value from the unheated sensor. Satellite rainfall, determined from various NWC-SAF products based on Meteosat data (see Section 2.3), showed only 0.05 mm/10 min (Fig.

13

394 8c); however, measurements based on data from visible and infrared channels are much less accurate than radar measurements.

395 The radar data confirmed that the rainfall that occurred in the analysed time step in the close vicinity of this rain station is

396 significantly higher than in the surroundings, but not by as much as the heated sensor reported – it is much closer to the

397 observation of the unheated sensor.

398   Visually, this conclusion seems to be unquestionable, but it may be interesting how the designed RainGaugeQC scheme

399 functioned in this situation.

400
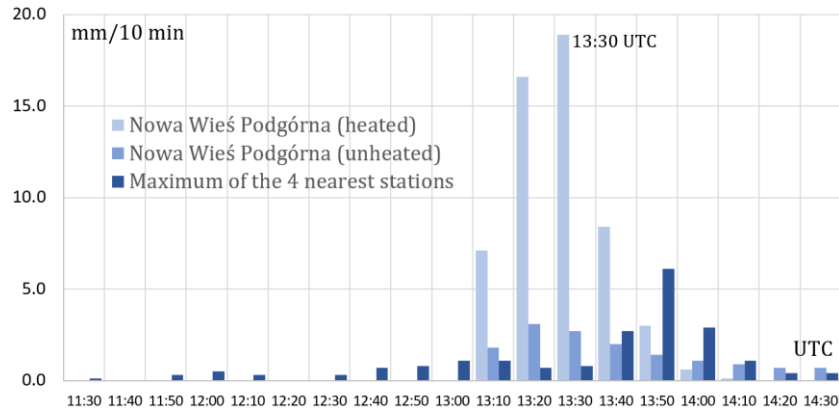
401

402 **Figure 9: Precipitation time series at Nowa Wieś Podgórna station in comparison to maximum of four neighbouring rain stations on**
403 **22 June 2021, from 11:30 to 14:30 UTC.**

404   Fig. 9 shows the recorded precipitation time series from 12 time steps (i.e. two hours) before the analysis date (13:30

405 UTC), and 6 time steps after this date, at Nowa Wieś Podgórna station (two sensors) and maximum values of the four

406 neighbouring stations. These stations are located between 19 and 35 km from the analysed Nowa Wieś Podgórna station. Until

407 the analysis date, precipitation measured by the sensors of these stations was not high, as it was up to about 1 mm/10 min, but

408 20 min later a significant increase in precipitation of about 6 mm/10 min was observed on both sensors of one of the nearby

409 stations. At the analysed time-step only Nowa Wieś Podgórna station recorded a slightly higher precipitation on the heated

410 sensor, while it was drastically higher on the unheated sensor (Table 2).

411

412 **Table 2. Results of QC of the Nowa Wieś Podgórna rain station on 22 June 2021, 13:30 UTC.**

Sensor	G (mm/10 min)	Check				QI (G) (–)
		RC	RSC	TCC	SCC	
Unheated	2.7	Passed	Passed	Failed	Weak outlier	0.75
Heated	18.9	Passed	Passed	Failed	Strong outlier	0.50

413

414   The quality of the data from this rain station was 0.75 for the G_{uh} sensor and 0.50 for G_h. This difference in QI values

415 was a result of the SCC test, which showed that the G_{uh} sensor differs slightly, and the G_h sensor differs significantly, from the

416 rainfall values in the neighbouring rain stations within the given subdomain. At the same time, both sensors failed the TCC

417 test, which in turn indicates that the accumulated values measured by these two sensors over the last 12 time steps differ

418 significantly (Table 2). This also contributed to a reduction in the final QI value.

419   Thus, finally, the value from the unheated sensor G_{uh} is taken for further processing. The precipitation field after the

420 spatial interpolation of QC data obtained by the ordinary kriging method is shown in Fig. 8d. The precipitation values around

421 this rain station location are clearly lower than those shown in Fig. 8a (without QC). The QI field for spatially interpolated rain

422 gauge data is shown in Fig. 8e – the Nowa Wieś Podgórna rain station is of lower quality than the neighbouring rain stations.

423   QC of rain gauge data influences the precipitation fields produced by applications for the generation of multi-source

424 fields. This is shown by the example of the QPE fields produced by the RainGRS system, which operationally combines

425 precipitation data from rain gauges, weather radar and meteorological satellites (see Section 2.3). In Fig. 8 two fields generated

by RainGRS are presented: based on rain gauge data without QC and after QC (Figs. 8f and 8g, respectively). Applying quality controlled rain gauge data, the RainGRS estimate decreases from 16.19 to 3.26 mm/10 min, which is a very significant effect.

4.4 General effects of the operation of the scheme

The performance of the RainGaugeQC scheme can be assessed by the degree of *QI* reduction. This is presented in Fig. 10, for individual months representative for autumn, winter, spring and summer conditions (October, January, April, and July, respectively).
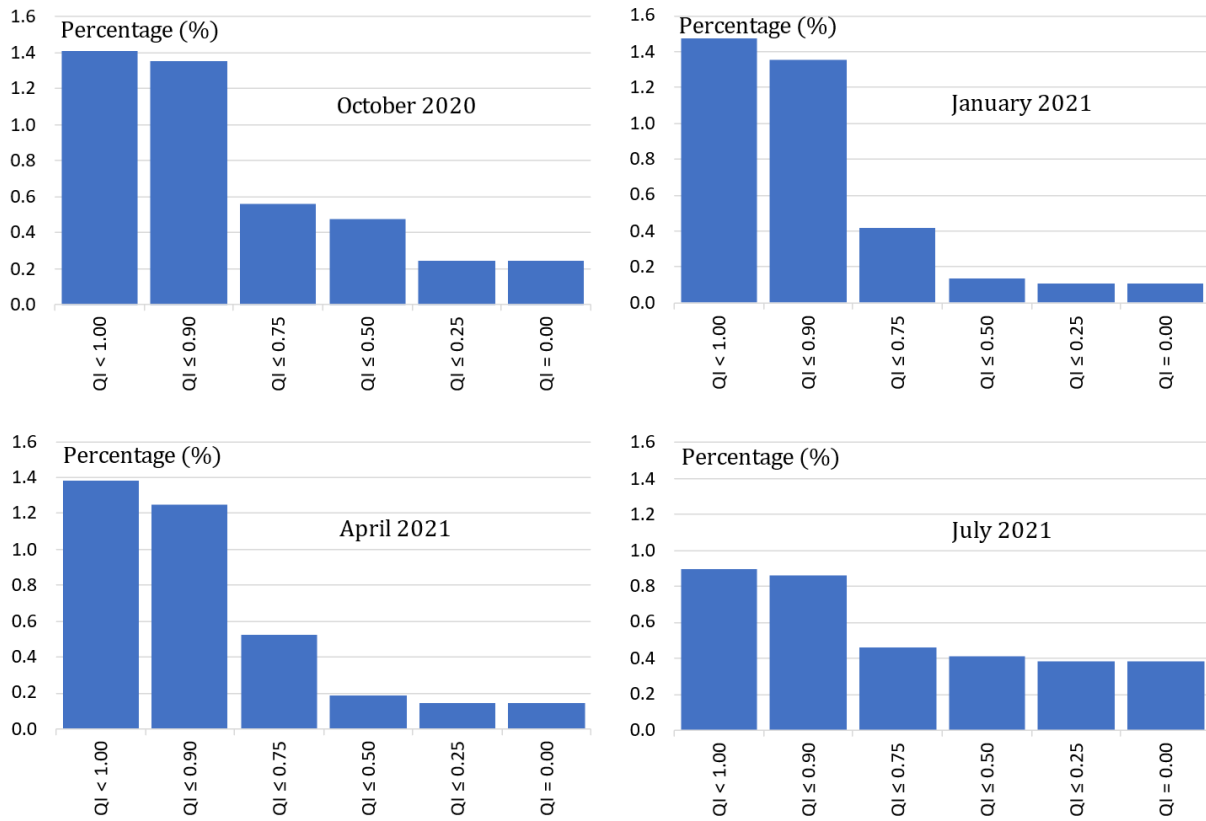
Figure 10: Percentage of rain gauge observations with a specified *QI* reduction after quality control. From top: percentage contribution in each *QI* interval; cumulative percentage contribution (in %); from left: October 2020, January, April, and July 2021.

The graphs shown do not include the percentage contribution of measurements that were assigned a quality of 1.0; this is equal to about 98.5–99.1%, much higher than the total contribution of all other values. In general, it can be seen from Fig. 10 that by far the greatest number of reductions in *QI* values was to values in the range (0.75, 0.90], and this is observed in all seasons of the year. Relatively large numbers of *QI* reductions to values in the range (0.50, 0.75] occur in winter (January) and spring (April), and relatively many data with quality reduced to zero value occur in summer (July) and autumn (October).

The number of rain gauge observations with reduced quality is relatively small, below 1.5%. For example, the contribution of data with *QI* reduced to zero (i.e. *QI* = 0.0) ranges from about one-third to one-tenth, but grows to about one-half over the summer (July). In practice, this means that these data were rejected. Probably the most important reason is that in the summer there often occurs convective precipitation, characterised by high intensities and strong spatial variability, and moreover rain gauges in no-rain situations react to morning dew condensation, which gives false rainfall measurements sometimes as high as 0.3 mm/10 min.

The most diverse distribution of *QI* reductions is observed in winter (January): most often there are small decreases in the *QI* value. In summer (July), this distribution is the least varied, which can be partially explained by the numerous *QI* reductions to zero.

15

5 Conclusions

1. Quality control of rain gauge data is essential, especially from the perspective of operational applications, when it is not possible to verify gauge data employing highly reliable precipitation measurements, such as manual Hellmann rain gauges, which are not available in real time.

2. It seems that the RainGaugeQC approach to the QC of rain gauge data, which consists in estimating the value of the *QI* of individual observations, enables more effective use of the data. On the one hand, it is a more cautious approach, as it does not eliminate all suspicious observations, and on the other hand, it enables flexible treatment of any suspected case of data incorrectness.

3. The IMGW rain station network consists mostly of rain stations equipped with two sensors: unheated and heated. This unique equipment allows the use of pairs of data to conduct much more effective QC. Comparing the observations from two sensors installed at the same location significantly increases the possibility of obtaining information about the uncertainty of measurements, for example by checking the time consistency of the data (TCC check). This is especially important when measurements are carried out with tipping bucket rain gauges, which have relatively low reliability. The availability of observations from both sensors is especially important during the warm season, when convective phenomena prevail. The frequent lack of two sensors installed at the same location reduces the scheme's effectiveness to some extent; however, it remains at a satisfactory level.

4. It is worth considering the possibility of employing radar data in the RCC and SCC algorithms to detect erroneous rain gauge measurements and to assess their reliability, based on the difference between the values from rain gauge and weather radar. The case study proved that the RainGaugeQC system can identify regionally inconsistent data thanks to the use of radar data as well as neighbouring rain gauge data.

5. The presented set of algorithms is based on empirical relationships that are strongly dependent on local conditions, both technical and geographic. The most important factors are the density of the rain station network, the availability of other data that can be used as a reference for QC (e.g. from the weather radar network), the type of sensors (their failure rate and measurement uncertainty), as well as terrain orography, wind conditions, and surface precipitation type. Therefore, any changes in the network configuration necessitate recalibration of the algorithms.

6. The number of rain gauge observations with reduced *QI* following QC under the RainGaugeQC scheme is relatively small, as it is below 1.5%. In all seasons, the highest number of *QI* value reductions was to values in the range [0.75, 0.90). The highest number of erroneous data (with *QI* reduced to zero) is found in summer (July) (approximately 0.4%), whereas in other seasons it ranges from about 0.10% to 0.23%.

Appendix 1. Detailed description of the Radar Conformity Check (RCC) algorithm

RCC is performed to identify false zero precipitation and false gauge-reported precipitation measurement by applying radar data.

1. Identifying false zero precipitation.
   Each gauge sensor value (*G*) less than 0.2 mm/10 min is checked against radar observations (*R*) at the gauge location and in its vicinity within a grid of 3 pixels x 3 pixels.

   If at least one pixel of radar data had precipitation above 0.4 mm/10 min, then the gauge value measured by this sensor is assumed to be erroneous, thus the sensor value is replaced by "no data" and the quality of this sensor is reduced to 0.

2. Identifying false gauge-reported precipitation.
   Each gauge sensor value (*G*) above 0 mm/10 min is checked against radar observations (*R*) at the gauge location and in its vicinity within a grid of 3 pixels x 3 pixels.

If at least two radar pixels with $QI > 0.85$ returned "no precipitation" ($R = 0$ mm/10 min), then the following conditions are checked:

(a) If for a given rain station, data are available only from one sensor (G) and $G > 0$ mm/10 min, then:
- if the station is located in a mountain or foothill area, the sensor is considered erroneous and its value is replaced by $G = 0$ mm and its quality reduced by 0.5;
- if the station is located in a lowland area, the sensor is considered erroneous and its value is replaced by $G = 0$ mm and its quality reduced by 0.25.

(b) If for a given rain station, data are available from two sensors (heated G_h and unheated G_{uh}) and $G_h > 0$ mm/10 min and $G_{uh} > 0$ mm/10 min, then:
- if the station is located in a mountain or foothill area and values from both sensors are similar, i.e. SF (G_{uh}, G_h) = "true", then the quality of both sensors is reduced by 0.75, but if SF (G_{uh}, G_h) = "false" then their qualities are reduced to $QI = 0$ and the sensor values are replaced by "no data";
- if the station is located in a lowland area, then the sensor qualities are reduced to $QI = 0$ and the sensor values are replaced by "no data".

(c) If for a given rain station, data are available from two sensors (heated G_h and unheated G_{uh}) and one of them reports "no precipitation" (i.e. $G_h = 0$ mm/10 min or $G_{uh} = 0$ mm/10 min), then:
- if the rain station is located in a mountain or foothill area and the values from both sensors are similar (i.e. SF (G_{uh}, G_h) = "true"), then the QI of the sensor which observed precipitation $G > 0$ mm/10 min is reduced by 0.75, but if SF (G_{uh}, G_h) = "false", then the QI of the sensor which reports $G > 0$ mm/10 min is reduced to $QI = 0$ and the sensor value is replaced by "no data";
- if the rain station is located in a lowland area, then the quality of the sensor that reports $G > 0$ mm/10 min is reduced to $QI = 0$ and the sensor value is replaced by "no data".

Appendix 2. Detailed description of the Temporal Conformity Check (TCC) algorithm

The first step of this check is performed to detect constant values observed by a given sensor. If the same value (e.g. 0.1 mm/10 min) is reported for a certain number of time steps (e.g. nine consecutive observations), then the sensor is probably clogged. In this case, the blocked sensor has failed the TCC test, its QI is reduced to 0, and the TCC test cannot be performed for the other sensor.

The main part of TCC serves to identify rain stations for which there are large differences between values measured simultaneously by pairs of rain sensors (G_h, G_{uh}), which may be evidence of their low quality. This check requires measurements from both rain gauge sensors at the same location; it can thus be conducted only in the warm season, when both sensors provide measurements. This lasts from April to October, when data from unheated sensors (G_{uh}) are available; the heated sensors (G_h) operate all year round.

1. Pairs of simultaneous measurements from two sensors are verified for the last 12 time steps, but observations with poor quality are not taken into account. If the number of quality-verified pairs (for previous time steps with $QI > 0.0$, and for the current one passing the previous checks, i.e. GEC, RC and RCC) is high enough (at least 9), the cumulative sums are calculated:

$$S_h = \sum_{i=1}^{n} G_{h,i}, \quad S_{uh} = \sum_{i=1}^{n} G_{uh,i} \tag{5}$$

2. The similarity of the accumulated sums is checked by means of the SF function. If they differ significantly, i.e. if $SF(S_h, S_{uh})$ = "false", then the data from both sensors have failed the TCC test and their quality is reduced by 0.25.

Appendix 3. Detailed description of the Spatial Consistency Check (SCC) algorithm

The SCC procedure consists of the following steps:

1. The Polish domain (900 km x 800 km) is divided into subdomains with dimensions of 100 km x 100 km. Only data with $QI > 0$ after previous tests are subject to this check. It is optional: (i) to analyse both sensors, heated and unheated, together or separately, (ii) to include also data from the previous time step (10 min ago) if their $QI = 1.0$. In order to perform this check there must be data available from at least three stations in a subdomain; otherwise the test is not performed for that subdomain.

2. Based on data from rain stations (G) located in a given subdomain, the following percentiles are determined: 25%, 50% (median), and 75% ($Q_{25}(G)$, $Q_{\mathrm{med}}(G)$, and $Q_{75}(G)$, respectively).

    The median absolute deviation (MAD) for a given subdomain is determined from the formula:

    $$MAD = \frac{1}{n}\sum_{i=1}^{n}|G_i - Q_{med}(G)| \tag{6}$$

    where n is the number of data, G_i is the i-th sensor value, and $Q_{\mathrm{med}}(G)$ is the median.

3. The index D_i, which determines numerically the deviation of the precipitation value measured with the i-th sensor from the median of all sensors within a given subdomain, is calculated from the formula (Kondragunta and Shrestha, 2006):

    $$D_i = \begin{cases} 0 & MAD = 0 \\ \dfrac{|G_i - Q_{med}(G)|}{MAD} & MAD \neq 0 \text{ and } Q_{75}(G) = Q_{25}(G) \\ \dfrac{|G_i - Q_{med}(G)|}{Q_{75}(G) - Q_{25}(G)} & MAD \neq 0 \text{ and } Q_{75}(G) \neq Q_{25}(G) \end{cases} \tag{7}$$

    Following calculation of the D_i values for all sensors within a given subdomain, three percentiles are determined: 90%, 95%, and 99% ($Q_{90}(D)$, $Q_{95}(D)$, and $Q_{99}(D)$, respectively).

4. If $D_i \leq Q_{90}(D)$, then the i-th sensor is not an outlier and the test is passed.

    If this is not the case, the i-th sensor is flagged and the formula (8) is applied to compare the index D_i with the three percentile values, in order to determine to which class of outliers the given value belongs:

    $$\text{outlier} = \begin{cases} \text{strong} & D_i > Q_{99}(D) \\ \text{medium} & Q_{95}(D) < D_i \leq Q_{99}(D) \\ \text{weak} & Q_{90}(D) < D_i \leq Q_{95}(D) \end{cases} \tag{8}$$

    The procedure is repeated in four subdomains resulting from shifting the given subdomain vertically (west-east) and horizontally (south-north), i.e. in four directions, with offsets of 25 km (except for subdomains on the edges and corners of the domain, which are shifted in three and two directions, respectively). If the value measured with a given sensor is flagged in all analysed subdomains, it fails the SCC check. If the values belonged to different classes of outliers, the weakest one is assigned to the sensor for further processing.

5. For sensors that failed the SCC check, if the data from both sensors are available for a given rain station and they are similar, i.e. $SF(G_h, G_{uh}) =$ "true", and passed the TCC check, then the QI for the sensor is not reduced.

    Otherwise, each outlier is verified against radar data. For this purpose the following values are determined within a grid of 5 pixels x 5 pixels around this rain station location: $\min(QI(R))$ – the minimum quality QI of the radar precipitation R; $R_{max} = \max(R: QI(R) > 0.75)$ – the maximum value of radar precipitation with a quality above 0.75; $QI(R_{\max})$ – the quality of the maximum value of radar precipitation R_{max}. This verification algorithm is as follows:

    If $\min(QI(R)) > 0.75$, then: $\tag{9}$

if $R_{max} = 0$, then the quality is reduced by 1.0 and G = "no data";

if $(G > 1.0 \text{ mm})$ and $\left(\frac{G}{R_{max}} < \frac{QI(R_{\max})}{4.0}\ \text{ or }\ \frac{G}{R_{max}} > \frac{4.0}{QI(R_{\max})}\right)$, then:

$$QI = \begin{cases} QI - 1.00 & \text{strong outlier} \\ QI - 0.50 & \text{medium outlier} \\ QI - 0.20 & \text{weak outlier} \end{cases}$$

if $(G > 1.0 \text{ mm})$ and $\left(\frac{G}{R_{max}} \geq \frac{QI(R_{\max})}{4.0}\ \text{ and }\ \frac{G}{R_{max}} \leq \frac{4.0}{QI(R_{\max})}\right)$, then:

$$QI = \begin{cases} QI - 0.25 & \text{strong outlier} \\ QI - 0.10 & \text{medium outlier} \\ QI & \text{weak outlier} \end{cases}$$

If $(G \leq 1.0 \text{ mm})$ or $\left(\min\big(QI(R)\big) \leq 0.75\right)$, then:

$$QI = \begin{cases} QI - 0.25 & \text{strong outlier} \\ QI - 0.10 & \text{medium outlier} \\ QI & \text{weak outlier} \end{cases}$$

where $\frac{4.0}{QI(R_{\max})}$ is the limitation to the magnitude of disparity $\frac{G}{R_{max}}$ determined empirically.

An alternative simplified analysis of the spatial consistency of rain gauge data may be performed analogously to steps 1–4, especially if radar data are unavailable. In this case, it is sufficient to determine only the $Q_{95}(D)$ percentile. Here, if in all subdomains $D_i > Q_{95}(D)$, the sensor fails the SCC, and the QI is decreased by 0.10.

References

Baserud, L., Lussana, C., Nipen, T.N., Seierstad, I.A., Oram, L., and Aspelien, T.: TITAN automatic spatial quality control of meteorological in-situ observations, Advances in Science and Research, 17, 153-163, https://doi.org/10.5194/asr-17-153-2020, 2020.

Bárdossy, A., Seidel, J., and El Hachem, A.: The use of personal weather station observation for improving precipitation estimation and interpolation, Hydrology and Earth System Sciences, 25, 583–601, https://doi.org/10.5194/hess-25-583-2021, 2021.

Blenkinsop, S., Lewis, E., Chan, S.C., and Fowler, H.J.: An hourly precipitation dataset and climatology of extremes for the UK. International Journal of Climatology, 37, 722–740, doi.org/10.1002/joc.4735, 2017.

Buisán, S. T., Earle, M. E., Collado, J. L., Kochendorfer, J., Alastrué, J., Wolff, M.. Smith, C. D., and López-Moreno, J. I.: Assessment of snowfall accumulation underestimation by tipping bucket gauges in the Spanish operational network, Atmospheric Measurement Techniques, 10, 1079–1091, https://doi.org/10.5194/amt-10-1079-2017, 2017.

Burszta-Adamiak, E., Licznar, P., and Zaleski, J.: Criteria for identifying maximum rainfall determined by the peaks-over-threshold (POT) method under the Polish Atlas of Rainfall Intensities (PANDa) project, Meteorology Hydrology and Water Management, 7, 3-13, https://doi.org/10.26491/mhwm/93595, 2019.

Colli, M., Lanza, L.G., and La Barbera P.: Performance of a weighing rain gauge under laboratory simulated time-varying reference rainfall rates, Atmospheric Research, 131, 3-12, https://doi.org/10.1016/j.atmosres.2013.04.006, 2013.

de Vos, L. W., Leijnse, H., Overeem, A., and Uijlenhoet, R.: Quality control for crowdsourced personal weather stations to enable operational rainfall monitoring, Geophysical Research Letters, 46, 8820–8829, https://doi.org/10.1029/2019GL083731, 2019.

Einfalt, T., Szturc, J., and Ośródka, K.: The quality index for radar precipitation data – a tower of Babel? Atmos. Sci. Lett., 11, 139-144. https://doi.org/10.1002/asl.271, 2010.

Fiebrich, C. A., Morgan, C. R., and McCombs, A. G.: Quality assurance procedures for mesoscale meteorological data. Journal of Atmospheric and Oceanic Technology, 27, 1565–1582, https://doi.org/10.1175/2010JTECHA1433.1, 2010.

Førland, E. J., Allerup, P., Dahlstrom, B., Elomaa, E., Jonsson, T., Madsen, H., Perala, H., Rissanen, P., Vedin, H., and Vejen, F.: Manual for operational correction of Nordic precipitation data. Report Nr 24/96. DNMI, Norway, pp. 66, 1996.

Golz, C., Einfalt, T., Gabella, M., and Germann, U.: Quality control algorithms for rainfall measurements, Atmospheric Research, 77, 247-255, https://doi.org/10.1016/j.atmosres.2004.10.027, 2005.

Goodison, B.E., Louie, P.Y.T., and Yang, D.: WMO solid precipitation measurement intercomparison: Final report, Instrum. Obs. Methods Rep. 67, World Meteorological Organization, Geneva, Switzerland. pp. 211, 1998.

Grossi, G., Lendvai, A., Giovanni Peretti, G., and Ranzi, R.: Snow precipitation measured by gauges: systematic error estimation and data series correction in the Central Italian Alps. Water, 9, 461, https://doi.org/10.3390/w9070461, 2017.

Habib, E., Krajewski, W., and Kruger, A.: Sampling errors of tipping-bucket rain gauge measurements, Journal of Hydrologic Engineering, 6, 159-166, https://doi.org/10.1061/(ASCE)1084-0699(2001)6:2(159), 2001.

Jurczyk, A., Szturc, J., Otop, I., Ośródka, K., and Struzik, P.: Quality-based combination of multi-source precipitation data, Remote Sensing, 12, 1709, https://doi.org/10.3390/rs12111709, 2020.

Kochendorfer, J., Earle, M. E., Hodyss, D., Reverdin, A., Roulet, Y.-A., Nitu, R., Rasmussen, R., Landolt, S., Buisan, S., and Laine, T.: Undercatch adjustments for tipping-bucket gauge measurements of solid precipitation, Journal of Hydrometeorology, 21, 1193–1205, https://doi.org/10.1175/JHM-D-19-0256.1, 2020.

Kondragunta, C. R. and Shrestha, K.: Automated real-time operational rain gauge quality-control tools in NWS Hydrologic Operations. 86th AMS Annual Meeting, Atlanta, GA, 28 January – 3 March 2006, 2006.

Lewis, E., Quinn, N., Blenkinsop, S., Fowler, H. J., Freer, J., Tanguy, M., Hitt, O., Coxon, G., Bates, P., and Woods, R.: A rule based quality control method for hourly rainfall data and a 1 km resolution gridded hourly rainfall dataset for Great Britain: CEH-GEAR1hr, Journal of Hydrology, 564, 930-943, https://doi.org/10.1016/j.jhydrol.2018.07.034, 2018.

Lewis, E., Pritchard, D., Villalobos-Herrera, R., Blenkinsop, S., McClean, F., Guerreiro, S., Schneider, U., Becker, A., Finger, P., Meyer-Christoffer, A., Rustemeier, E., and Fowler, H. J.: Quality control of a global hourly rainfall dataset, Environmental Modelling & Software, 144, 105169, https://doi.org/10.1016/j.envsoft.2021.105169, 2021.

Martinaitis, S. M., Cocks, S. B., Qi, B., Kaney, Y., Zhang, J., and Howard, K.: Understanding winter precipitation impacts on automated gauges within a real-time system, Journal of Hydrometeorology, 16, 2345-2363, https://doi.org/10.1175/JHM-D-15-0020.1, 2015.

Michelson, D.: Systematic correction of precipitation gauge observations using analyzed meteorological variables, Journal of Hydrology, 290, 161–177, https://doi.org/10.1016/j.jhydrol.2003.10.005, 2004.

Moslemi, M. and Joksimovic, D.: Real-time quality control and infilling of precipitation data using neural networks, EPiC Series in Engineering (HIC 2018. 13th International Conference on Hydroinformatics), 3, 1457-1464, https://doi.org/10.29007/t5k7, 2018.

Neuper, M. and Ehret, U.: Quantitative precipitation estimation with weather radar using a data- and information-based approach, Hydrology and Earth System Sciences, 23, 3711–3733, https://doi.org/10.5194/hess-23-3711-2019, 2019.

Niu, G., Yang, P., Zheng, Y., Cai, X., and Qin, H.: Automatic quality control of crowdsourced rainfall data with multiple noises: A machine learning approach, Water Resources Research, 57, e2020WR029121, https://doi.org/10.1029/2020WR029121, 2021.

Ośródka, K., Szturc, J., and Jurczyk A.: Chain of data quality algorithms for 3-D single-polarization radar reflectivity (RADVOL-QC system), Meteorological Applications, 21, 256-270, https://doi.org/10.1002/met.1323, 2014.

Ośródka, K. and Szturc, J.: Improvement in algorithms for quality control of weather radar data (RADVOL-QC system), Atmospheric Measurement Techniques, 15, 261-277, https://10.5194/amt-15-261-2022, 2022.

Otop, I., Szturc, J., Ośródka, K. and Djaków, P.: Automatic quality control of telemetric rain gauge data for operational applications at IMGW-PIB, ITM Web Conf., 23, 00028, https://doi.org/10.1051/itmconf/20182300028, 2018.

Qi, Y., Martinaitis, S., Zhang, J., and Cocks, S.: A real-time automated quality control of hourly rain gauge data based on multiple sensors in MRMS System, Journal of Hydrometeorology, 17, 1675-1691, https://doi.org/10.1175/JHM-D-15-0188.1, 2016.

Rasmussen, R., Baker, B., Kochendorfer, J., Meyers, T., Landolt, S., Fischer, A. P., Black, J., Theriault, J. M., Kucera, P., Gochis, D., Smith, C., Nitu, R., Hall, M., Ikeda, K., and Gutmann, E.: How well are we measuring snow? The NOAA/FAA/NCAR winter precipitation Test Bed, Bulletin of the American Meteorological Society, 93, 811-829, https://doi.org/10.1175/BAMS-D-11-00052.1, 2012.

Savina, M., Schappi, B., Molnar, P., Burlando, P., and Sevruk, B.: Comparison of a tipping-bucket and electronic weighing precipitation gauge for snowfall, Atmospheric Research, 103, 54-51, https://doi.org/10.1016/j.atmosres.2011.06.010, 2012.

Scherrer, S. C., Frei, C., Croci-Maspoli, M., van Geijtenbeek, D., Hotz, C., and Appenzeller C.: Operational quality control of daily precipitation using spatio-climatological plausibility testing, Meteorologische Zeitschrift, 20, 397-407, https://doi.org/10.1127/0941-2948/2011/0236, 2011.

Sevruk, B.: Adjustment of tipping-bucket precipitation gauge measurements, Atmospheric Research, 42, 237-246, https://doi.org/10.1016/0169-8095(95)00066-6, 1996.

Sevruk, B. and Nevenic, M.: The geography and topography effects on the areal pattern of precipitation in a small prealpine basin, Water Science and Technology, 37, 163-170,1998.

Sevruk, B., Ondras M., and Chvila B.: The WMO precipitation intercomparisons, Atmospheric Research, 92, 376-380, https://doi.org/10.1016/j.atmosres.2009.01.016, 2009.

Shedekar, V. S., King, K. W., Fausey, N. R., Soboyejo, A. B. O., Harmel, R. D., and Brown, L. C.: Assessment of measurement errors and dynamic calibration methods for three different tipping bucket rain gauges, Atmospheric Research, 178, 445-458, https://doi.org/10.1016/j.atmosres.2016.04.016, 2016.

Sieck, L.C., Burges, S. J. and Steiner, M.: Challenges in obtaining reliable measurements of point rainfall, Water Resources Research, 43, W01420, https://doi.org/10.1029/2005WR004519, 2007.

Steinacker, R., Mayer, D., Steiner, A.: Data quality control based on self-consistency, Monthly Weather Review, 139, 3974–3991, https://doi.org/10.1175/MWR-D-10-05024.1, 2011.

Szturc, J., Jurczyk, A., Ośródka, K., Wyszogrodzki, A., and Giszterowicz, M.: Precipitation estimation and nowcasting at IMGW (SEiNO system), Meteorology Hydrology and Water Management, 6, 3–12, https://doi.org/10.26491/mhwm/76120, 2018.

Szturc, J., Ośródka, K., Jurczyk, A., Otop, I., Linkowska, J., Bochenek, B., and Pasierb, M.: Quality control and verification of precipitation observations, estimates, and forecasts, in: Precipitation Science. Measurement, Remote Sensing, Microphysics and Modeling, Michaelides, S., edited by: Elsevier 2022, 91-133, https://doi.org/10.1016/B978-0-12-822973-6.00002-0, 2022.

Taylor, J. R. and Loescher, H. L.: Automated quality control methods for sensor data: a novel observatory approach, Biogeosciences, 10, 4957-4971, https://doi.org/10.5194/bg-10-4957-2013, 2013.

Upton, G. and Rahimi A.: On-line detection of errors in tipping-bucket raingauges, Journal of Hydrology, 278, 197-212, https://doi.org/10.1016/S0022-1694(03)00142-2, 2003.

685 Urban, G. and Strug, K.: Evaluation of precipitation measurements obtained from different types of rain gauges,
686   Meteorologische Zeitschrift, 30, 445-463, https://doi.org/10.1127/metz/2021/1084, 2021.

687 Villalobos Herrera, R., Blenkinsop, S., Guerreiro, S. B., O'Hara, T., Fowler, H. J.: Sub-hourly resolution quality control of
688   rain gauge data significantly improves regional sub-daily return level estimates, Quarterly Journal of the Royal
689   Meteorological Society (submitted), 2022.

690 WMO-No. 8: Guide to Instruments and Methods of Observation, vol. I: Measurement of Meteorological Variables, 2018
691   edition. World Meteorological Organization, Geneva, pp. 548., 2018.

692 WMO-No. 305: Guide on the Global Data-processing System, 1993 edition. World Meteorological Organization, Geneva, pp.
693   199, 1993.

694 WMO-No. 488: Guide to the Global Observing System, 2010 edition, updated in 2017. World Meteorological Organization,
695   Geneva, pp. 215, 2017.

696 Yeung, H.Y., Man, C., Chan S.T., and Seed, A.: Development of an operational rainfall data quality-control scheme based on
697   radar-raingauge co-kriging analysis, Hydrological Sciences Journal, 59, 1293-1307,
698   https://doi.org/10.1080/02626667.2013.839873, 2014.

699 You, J., Hubbard K. G., Nadarajah S., and Kunkel K. E.: Performance of quality assurance procedures on daily precipitation,
700   Journal of Atmospheric and Oceanic Technology, 24, 821-834, https://doi.org/10.1175/JTECH2002.1, 2007.

701